Oleylamine-Stabilized Palladium(0) Nanoclusters As Highly Active Heterogeneous Catalyst for the Dehydrogenation of Ammonia Borane

ARTICLE *in* THE JOURNAL OF PHYSICAL CHEMISTRY C · APRIL 2011

Impact Factor: 4.77 · DOI: 10.1021/jp201906n

4 AUTHORS:

Onder Metin
Ataturk University
55 PUBLICATIONS **1,527** CITATIONS
SEE PROFILE

Sibel Duman
Bingöl University
12 PUBLICATIONS **57** CITATIONS
SEE PROFILE

Melek Dinc
Middle East Technical University
4 PUBLICATIONS **82** CITATIONS
SEE PROFILE

Saim Özkar
Middle East Technical University
298 PUBLICATIONS **5,265** CITATIONS
SEE PROFILE

THE JOURNAL OF PHYSICAL CHEMISTRY C

ARTICLE

pubs.acs.org/JPCC

Oleylamine-Stabilized Palladium(0) Nanoclusters As Highly Active Heterogeneous Catalyst for the Dehydrogenation of Ammonia Borane

Önder Metin,[†] Sibel Duman,[‡] Melek Dinç, and Saim Özkar*

Department of Chemistry, Middle East Technical University, 06531 Ankara, Turkey

ABSTRACT: Palladium(0) nanoclusters having an average particle size of 3.2 nm were generated in situ from the reduction of palladium(II) acetylacetonate in the presence of oleylamine (OAm) during the dehydrogenation of ammonia−borane (AB) in THF under inert gas atmosphere at room temperature. OAm-stabilized palladium(0) nanoclusters were stable enough to be isolated as solid materials and characterized by TEM, HRTEM, XRD, UV−vis, and FT-IR techniques. They were found to be highly active catalysts in the hydrogen generation from the dehydrogenation of AB; in total, 2 equiv of hydrogen gas per AB was generated even at low catalyst concentration and room temperature. The first and second equivalent of H_2 generation from AB were completed in ∼20 and 100 min, respectively, from the dehydrogenation of AB in the presence of palladium(0) nanoclusters corresponding to an initial turnover frequency of 240 h^{-1}. ^{11}B NMR study of the reaction shows that hydrogen evolution likely takes place in one or both of two parallel routes: (i) through formation of cyclopolyborazane followed by its polymerization to polyborazylene and (ii) through formation of long-chain B−N linear polymers. Carbon disulfide poisoning experiments indicate that the dehydrogenation of AB catalyzed by OAm-stabilized palladium(0) nanoclusters is heterogeneous catalysis. Moreover, the work reported here includes a wealthy collection of kinetic data to determine the rate law and apparent activation energy for the catalytic dehydrogenation of AB.

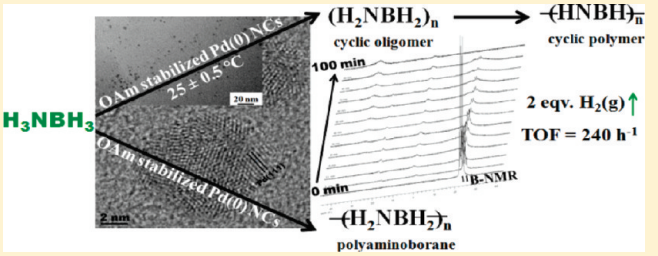

1. INTRODUCTION

A practical hydrogen generator combined with an efficient fuel cell is still needed for the utility of hydrogen as an energy carrier for mobile applications.[1,2] One conceptual solution is the generation of hydrogen from solid hydrogen storage materials having high gravimetric hydrogen storage capacity such as boron−nitrogen compounds.[3] Among these materials, ammonia−borane (H_3NBH_3, AB) has received increasing attention owing to its impressive gravimetric hydrogen content of 19.6 wt % (6.5 and 13.1 wt % for the first and second equivalents of H_2, respectively), stability in the solid state under ambient conditions, and nontoxicity.[4] Thus far, hydrogen generation from AB has been achieved by thermolysis,[5] solvolysis (hydrolysis or methanolysis),[6,7] and dehydrogenation.[8] The high temperature requirement of the thermolysis for release of 3 equiv of hydrogen (around 1400 °C)[9] and difficulties in the regeneration of solvolysis products due to the strong B−O bonds make the dehydrogenation route most promising. Moreover, recent reports related to the regeneration of the dehydrogenation products amplify the importance of the catalytic dehydrogenation of AB to supply hydrogen for portable applications.[10] However, dehydrogenation of AB is a harsh reaction and only takes place in the presence of a suitable catalyst.

Many transition metal catalysts have been tested for AB dehydrogenation, but most of them lack the desired efficiency and produce less than 2 equiv of hydrogen gas in a very long reaction time.[11] In this regard, thus far, several efficient catalyst systems have been reported involving rhodium,[12] iridium,[13] ruthenium,[14] and nickel.[15] As a common feature, all of these catalytic systems, except the in-situ-formed unstable $Rh(0)_n$ species,[11] involve homogeneous catalysis. In a recent study, a highly active homogeneous palladium catalyst, $[Pd(allyl)][BF_4]$, has been reported for the dehydrogenation of AB, releasing 2 equiv of H_2 in less than 60 s at room temperature corresponding to an initial turnover frequency of 4000 h^{-1}, the best among all the catalyst systems ever reported for the dehydrogenation of AB at room temperature.[16] Despite its superb activity, the homogeneous $[Pd(allyl)][BF_4]$ catalyst is not stable and precipitates out together with the insoluble reaction products after the first cycle of AB dehydrogenation. Although the $[Pd(allyl)][BF_4]$ complex has been the first example of homogeneous palladium catalysts in the dehydrogenation of AB, there exists only one heterogeneous palladium catalyst reported for the same reaction, namely, the commercial 10% Pd on carbon,[17] which has been found to show very low activity, generating less than 0.4 equiv of H_2 in the dehydrogenation of AB even at 70 °C. As the activity of heterogeneous catalysts is directly related to surface area, reduction of the particle size of the heterogeneous catalyst is a promising way to increase the catalytic activity.[18] An efficient way of increasing catalytic activity is the use of metal nanoclusters which are more active catalysts than the respective bulk metal, because a large percentage of atoms are on the surface of nanoclusters.[19,20] In this context, our recent paper has reported that rhodium(0)

Received: February 27, 2011
Revised: April 21, 2011

   dx.doi.org/10.1021/jp201906n | J. Phys. Chem. C XXXX, XXX, 000–000

nanoparticles stabilized by *tert*-butylammonium octanoate are highly active catalysts in the dehydrogenation of AB at room temperature.[21] Herein, we report that the in-situ-generated palladium(0) nanoclusters, stabilized by oleylamine, are highly active and stable heterogeneous catalysts in the dehydrogenation of AB at room temperature. Palladium(0) nanoclusters are generated in situ from the reduction of palladium(II) acetylacetonate in the presence of oleylamine (OAm) during the dehydrogenation of AB in THF under inert gas atmosphere at room temperature. A rapid hydrogen generation starts immediately, and concomitant color change from pale yellow to dark brown indicates formation of OAm-stabilized palladium(0) nanoclusters. Oleylamine has been shown to stabilize a variety of transition metal nanoparticles including palladium.[22] The OAm-stabilized palladium(0) nanoclusters were characterized by transmission electron microscopy (TEM), high-resolution TEM (HRTEM), UV−visible electronic absorption spectroscopy, FTIR spectroscopy, and X-ray diffraction (XRD). The heterogeneity of the in-situ-generated palladium(0) nanoclusters in the dehydrogenation of AB was identified by carbon disulfide poisoning experiments. Two equivalents of hydrogen gas per AB were generated from the dehydrogenation catalyzed by palladium(0) nanoclusters. The first and second equivalent of H_2 release from AB were achieved in ∼20 and 100 min, respectively, in the presence of 2.5 mM Pd corresponding to an initial turnover frequency of 240 h^{-1} at room temperature. The catalytic dehydrogenation of AB in the presence of palladium(0) nanoclusters was also followed by ^{11}B NMR spectroscopy. Our report also includes the detailed kinetics of dehydrogenation of AB depending on the catalyst concentration, substrate concentration, and temperature.

2. EXPERIMENTAL SECTION

Materials. All commercially obtained chemicals were used as received unless indicated otherwise. Palladium(II) acetylacetonate (99%), oleylamine (OAm, >70%), borane ammonia complex (AB, 97%), hexane (99%), pure carbon disulfide, and deuterated chloroform were purchased from Sigma-Aldrich. Tetrahydrofuran (THF) was purchased from Fluka and distilled over sodium−benzophenone mixture under a nitrogen atmosphere for 12 h. All glassware and Teflon-coated magnetic stir bars were cleaned with acetone, followed by copious rinsing with distilled water before drying at 150 °C in an oven overnight.

Instrumentation. Transmission electron microscope (TEM) images were obtained using a JEM-2100 (JEOL) instrument operating at 200 kV. A very dilute solution of OAm-stabilized palladium(0) nanoclusters was prepared in THF or hexane, and 1 drop of this solution was placed on the copper grid. Samples were examined at magnification between 100 and 800 K. UV−vis electronic absorption spectra were recorded on a Shimadzu-2450 UV−vis−NIR double-beam spectrophotometer. The X-ray diffraction pattern (XRD) was recorded on a Rigaku Miniflex diffractometer with Cu Kα (30 kV, 15 mA, λ = 1.54051 Å), over a 2θ range from 5° to 90° at room temperature. The ^{11}B NMR spectrum was measured on a Bruker Avance DPX 400 MHz spectrometer (400.1 MHz for ^{1}H NMR; 100.6 MHz for ^{13}C NMR; 128.2 MHz for ^{11}B NMR). $BF_3 \cdot (C_2H_5)_2O$ was used as the external reference for ^{11}B NMR chemical shifts. The infrared spectrum was recorded from a Vertex 70 ATR/FTIR spectrometer.

In-Situ Generation of Oleylamine-Stabilized Palladium(0) Nanoclusters and Concomitant Dehydrogenation of AB. All reactions and manipulations were performed under a dry nitrogen atmosphere using standard Schlenk techniques including a vacuum system unless otherwise specified. Both the in-situ generation of OAm-stabilized palladium(0) nanoclusters and the concomitant dehydrogenation of AB were performed in a typical jacketed, three-necked reaction flask connected to the water-filled cylinder glass tube. The jacketed reaction flask was kept under vacuum at least for 15 min and filled with nitrogen to remove any trace of oxygen and water present before all catalytic reactions. The catalytic activity of palladium(0) nanoclusters in the dehydrogenation of AB was determined by measuring the rate of hydrogen generation. A stock solution of 8.0 mM oleylamine was prepared by dissolving 0.019 mL of OAm (MW = 267.5 $g \cdot mol^{-1}$, d = 0.813 $g \cdot mL^{-1}$, 70 wt %) in 5.0 mL of THF. Next, 2.3 mg (0.01 mmol) of palladium(II) acetylacetonate was dissolved in an aliquot of the OAm stock solution that was diluted to the desired volume by THF to obtain the OAm−Pd mixture at a molar ratio in the range of 4.0−12.0. In a vial 31.0 mg (1.0 mmol) of AB was dissolved in 4.0 mL of THF. The solution was transferred into the jacketed reaction flask thermostatted at 25.0 ± 0.5 °C. Then, a 1.0 mL aliquot of the OAm−Pd solution was injected via a gastight syringe into the reaction flask under vigorous stirring. The abrupt color change from yellow to dark brown indicates formation of OAm-stabilized palladium(0) nanoclusters, and hydrogen gas evolution starts immediately. Hydrogen gas generation from the catalytic reaction solution was followed using a typical water-filled gas buret system and recording the displacement of the water level in the gas buret every minute until no more hydrogen evolution was observed. When no more hydrogen generation was observed, the experiment was stopped, the reactor was disconnected from the water-filled tube, and the hydrogen pressure was released. Next, an approximately 0.5 mL aliquot of the reaction solution in the reactor was withdrawn with a glass Pasteur pipet and added to 1 g of $CDCl_3$ in a quartz NMR sample tube (Norell S-500-QTZ), which was subsequently sealed. The ^{11}B NMR spectrum of this solution showed complete conversion of H_3NBH_3 (quartet at −23 ppm) to products, giving peaks at 1.0, 17.0, and 26.0 ppm. Additionally, no bulk metal formation was observed during the catalytic dehydrogenation reaction, and the nanoclusters were very stable in THF solution even for months.

Effect of Oleylamine Concentration on the Catalytic Activity of Palladium(0) Nanoclusters in the Dehydrogenation of AB. In order to study the effect of OAm concentration on the catalytic activity of palladium(0) nanoclusters in the dehydrogenation of AB (100 mM), catalytic activity tests were performed at 25.0 ± 0.5 °C starting with various concentrations of OAm (1.0, 2.0, 3.0, 4.0, 5.0, and 10.0 mM) at constant palladium(II) acetylacetonate concentration (1.0 mM). In all experiments, the total volume of the solution was kept constant at 5.0 mL. All experiments were performed in the same way as described in the section In-situ Generation of Oleylamine-Stabilized Palladium(0) Nanoclusters and Concomitant Dehydrogenation of AB. The high stability and highest activity of OAm-stabilized palladium(0) nanoclusters in the dehydrogenation of AB were achieved at a OAm to palladium ratio of 4. Thus, the OAm concentration of 8.0 mM, corresponding to a OAm to palladium ratio of 4, was selected for further experiments.

Kinetics of Dehydrogenation of AB Catalyzed by Oleylamine-Stabilized Palladium(0) Nanoclusters. In order to establish the rate law and obtain the activation parameters for the catalytic dehydrogenation of AB in the presence of palladium(0)

dx.doi.org/10.1021/jp201906n |*J. Phys. Chem. C* XXXX, XXX, 000–000

nanoclusters stabilized by OAm, three different sets of experiment were performed in the same ways described in the section In-Situ Generation of Oleylamine-Stabilized Palladium(0) Nanoclusters and Concomitant Dehydrogenation of AB. In the first set of experiments, the concentration of AB was kept constant at 200.0 mM and palladium concentration was varied in the range of 1.0, 1.5, 2.0, 2.5, and 3.0 mM at 25 ± 0.5 °C. In the second set of experiments, the palladium concentration was held constant at 2.0 mM Pd while AB concentration was varied in the range of 100, 150, 200, 250, and 300 mM at 25 ± 0.5 °C. Finally, the catalytic dehydrogenation of AB was performed in the presence of the OAm-stabilized palladium(0) nanoclusters at constant AB (200.0 mM) and palladium concentration 2.0 mM at various temperatures in the range of 20−40 °C in order to obtain the apparent activation energy ($E_{a^{app}}$). In all kinetic experiments, a 4-fold amount of OAm per palladium was added into the catalytic reaction solution considering the optimum stability and activity of the nanoclusters. The volume of hydrogen versus time data was processed using Origin 8.0 software.

Determination of the Catalytic Lifetime of Oleylamine-Stabilized Palladium(0) Nanoclusters in the Dehydrogenation of AB. The catalytic lifetime of in-situ-generated OAm-stabilized palladium(0) nanoclusters in the dehydrogenation of AB was determined by measuring the total turnover number (TTON). Such a lifetime experiment was started with a 5.0 mL solution containing 1.0 mM Pd and 200.0 mM AB at 25 ± 0.5 °C. When all the AB present in the solution was consumed by checking stoichiometric H_2 gas evolution (2.0 mol H_2/mol H_3NBH_3) a new batch of AB was added, and the reaction was continued in this way until no hydrogen gas evolution.

CS_2 Poisoning Test for the Heterogeneity of Oleylamine-Stabilized Palladium(0) Nanoclusters in the Dehydrogenation of AB. The ability of CS_2 to poison metal−particle heterogeneous catalyst by adsorbing on the metal surface has been proposed in reducing reaction medium. In a typical poisoning experiment, 2.0 mM in-situ-generated OAm-stabilized palladium(0) nanoclusters having a OAm/Pd molar ratio of 4 in 5.0 mL of 200 mM AB solution at 25.0 ± 0.5 °C was poisoned by adding 0.1 equiv of CS_2 per palladium solution prepared in THF after 50% conversion. The catalytic activity was measured by monitoring the rate of hydrogen generation before and after addition of CS_2.

3. RESULTS AND DISCUSSION

In-Situ Generation and Characterization of Oleylamine-Stabilized Palladium(0) Nanoclusters. Palladium(0) nanoclusters formed in situ from the reduction of palladium(II) acetylacetonate in the presence of OAm during the dehydrogenation of AB are highly stable in THF at room temperature. For example, no bulk metal formation was observed in solution standing for months under inert gas atmosphere at room temperature. Additionally, these palladium(0) nanoclusters can be isolated from the reaction solution via centrifugation by ethanol addition and redispersed in a variety of apolar solvents such as hexane and toluene.

Reduction of palladium(II) acetylacetonate and formation of palladium(0) nanoclusters were nicely followed by UV−vis electronic absorption spectroscopy. Figure 1 shows the UV−vis spectra of solutions containing palladium(II) acetylacetonate in the presence of OAm in THF before and after its injection into the AB solution. The UV−vis spectrum of palladium(II) acetylacetonate in the presence of OAm in THF has two absorption

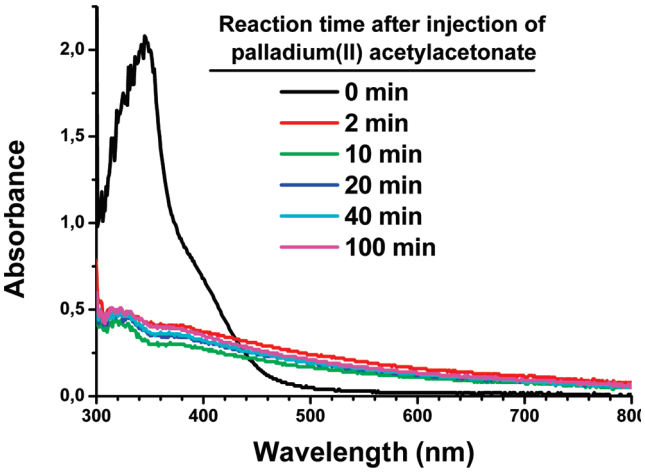

Figure 1. UV−vis electronic absorption spectra of a solution containing palladium(II) acetylacetonate in the presence of OAm in THF before and after its injection into the AB at certain time intervals.

bands at 345 and 408 nm, attributable to the charge transfer and d−d transitions, respectively. After its injection into the AB solution, these bands disappear and one observes a typical Mie scattering spectrum indicating reduction of palladium(II) acetylacetonate and formation of palladium(0) nanoclusters stabilized by OAm, consistent with earlier studies.[23,24]

The morphology and particle size of OAm-stabilized palladium(0) nanoclusters were studied by TEM. Figure 2a and 2b shows the TEM images taken either directly from the reaction solution or after centrifugation by ethanol addition and redispersing in hexane, respectively. The TEM image directly taken from the reaction solution (Figure 2a) shows that the OAm-stabilized palladium(0) nanoclusters with an average particle size of 3.2 ± 1.2 nm are formed in reaction solution. A similar average particle size of 3.4 ± 1.0 nm was calculated from the TEM image of the OAm-stabilized palladium(0) nanoclusters isolated and redispersed in hexane. This indicates the capability of oleylamine in stabilizing the palladium(0) nanoparticles and redispersibility of palladium(0) nanoparticles in different apolar organic solvents such as hexane.

Powder-XRD and HR-TEM analyses were used to investigate the crystallinity of the OAm-stabilized palladium(0) nanoclusters. Figure 3 shows the XRD pattern of OAm-stabilized palladium(0) nanoclusters generated in situ during the dehydrogenation of AB. Four reflections in the XRD pattern at 2θ = 40°, 46°, 68°, and 82° are attributed to the 111, 200, 220, and 311 planes of a face-centered cubic (fcc) crystal structure of palladium, respectively.[25] A high-resolution TEM study of a series of single palladium(0) nanoclusters indicates that the as-prepared palladium(0) nanoclusters have a polycrystalline structure (Figure 4), but the (111) planes can still be identified by the typical interfringe distance of 0.221 nm, which is close to the lattice spacing of the (111) planes of the fcc palladium (0.223 nm). By using the Debye−Scherrer formula an average particle size of 2.95 nm was estimated from the XRD patterns, which is smaller than the average value of 3.2 and 3.4 nm calculated from the TEM images in Figure 2a and 2b, respectively.[22,26] This small mismatch in XRD crystallite size and HR-TEM dimension reflects the polycrystalline nature of the palladium(0) nanoclusters.[27]

The integrity of the OAm on the stabilization of palladium(0) nanoclusters was examined by ATR-FTIR spectroscopy.

dx.doi.org/10.1021/jp201906n |J. Phys. Chem. C XXXX, XXX, 000–000

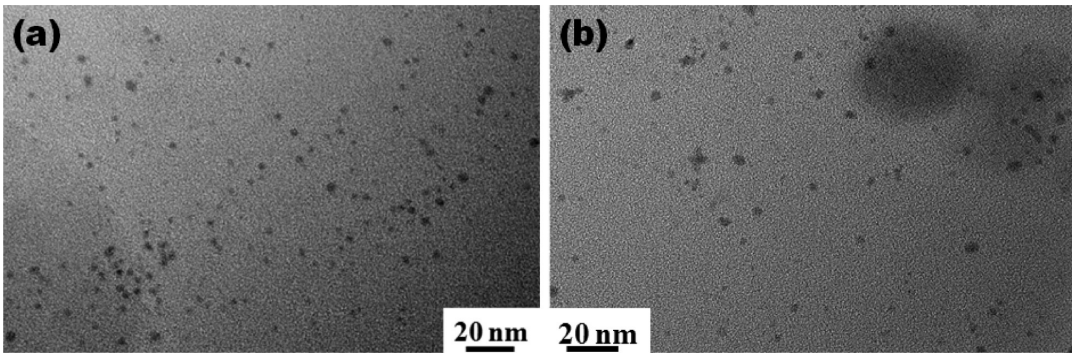

Figure 2. TEM images taken (a) directly from the reaction solution and (b) after centrifugation by ethanol addition and redispersing in hexane.

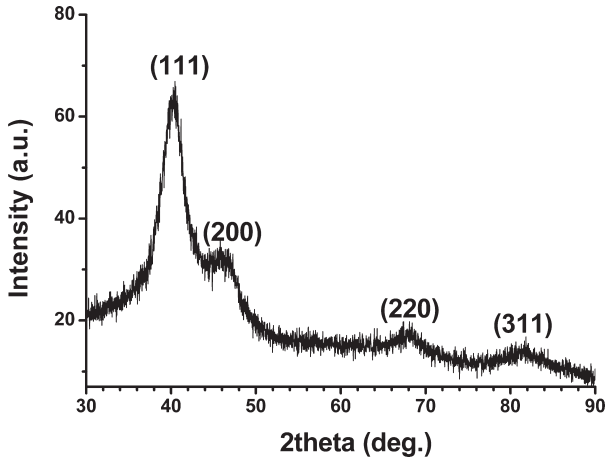

Figure 3. XRD pattern of OAm-stabilized palladium(0) nanoclusters generated in situ during the dehydrogenation of AB at room temperature.

The presence of the OAm in the nanoclusters sample, most probably adsorbed on the surface, was concluded by comparing the IR spectra of neat OAm and the OAm-stabilized palladium(0) nanoclusters sample.

Dehydrogenation of AB Catalyzed by Oleylamine-Stabilized Palladium(0) Nanoclusters. The progress of the dehydrogenation of AB in the presence of the OAm-stabilized palladium(0) nanoclusters was followed by measuring the volume of hydrogen generated (Figure 5) and analyzing the reaction products by ^{11}B NMR spectroscopy (Figure 6). Since the reduction of palladium(II) ions and formation of palladium(0) nanoparticles are very fast, as observed by the UV−vis electronic absorption spectroscopy, a fast hydrogen generation starts immediately without an induction period in the dehydrogenation of ammonia borane (Figure 5). Palladium(0) nanoclusters are highly active catalysts in the dehydrogenation of AB; in total, 2 equiv of hydrogen gas per AB are generated even at low catalyst concentration (1.0 mM Pd) and room temperature. The first and second equivalent of H_2 generation from AB are completed in ~20 and 100 min, respectively, from the dehydrogenation of AB in the presence palladium(0) nanoclusters (2.5 mM Pd). The initial turnover frequency of catalytic dehydrogenation was measured to be 240 h^{-1} at 25 ± 0.5 °C. This TOF value is one of the highest ever reported for the catalyst systems in the dehydrogenation of AB,[28] and this is the first example of using palladium(0) nanoclusters as catalyst for the dehydrogenation of

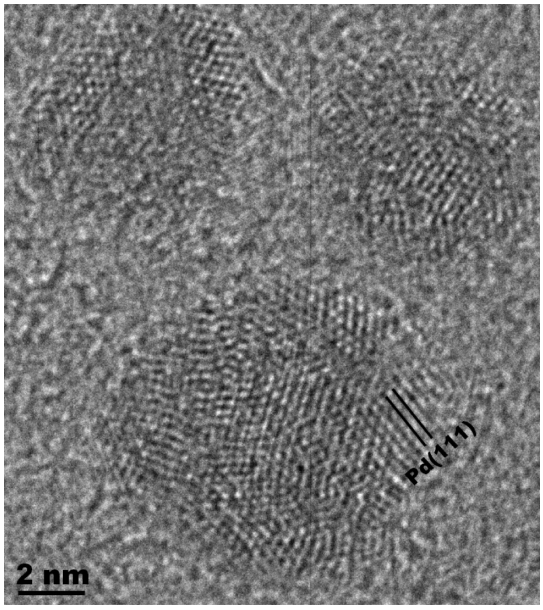

Figure 4. HRTEM image of in-situ-generated OAm-stabilized palladium(0) nanoclusters taken from hexane solution of the nanoclusters after centrifugation by ethanol addition.

AB at room temperature. Progress of the dehydrogenation of AB catalyzed by OAm-stabilized palladium(0) nanoclusters was followed by ^{11}B NMR spectroscopy at 25 ± 0.5 °C. Figure 6 shows the ^{11}B−{^{1}H} NMR spectra obtained at different reaction times in the range of 0−100 min. As the reaction proceeds, the resonance signal of ammonia borane (quarted at −23 ppm) gradually loses intensity and ultimately disappears in 100 min while resonance signals for the dehydrogenation products grow in. Two signals first grow in at 1.0 and 17.0 ppm attributed to B−N linear polymers and cyclopolyborazane, respectively.[3,29] After 40 min, a new signal starts to grow in at 26.0 ppm attributed to polyborazylene with a concomitant decrease in intensity of the peak at 17.0 ppm, indicating polymerization of cyclopolyborazane to polyborazylene, which is known to be the ultimate product when 2 equiv of H_2 is released.[30] That the signal at 1.0 ppm retains its intensity until the end of reaction is due to the limited solubility of the linear B−N polymers in THF. In light of these results, it can be concluded that dehydrogenation of AB catalyzed by OAm-stabilized palladium(0) nanoclusters can release 2 equiv of H_2 following one of two parallel routes: (i) through

dx.doi.org/10.1021/jp201906n |J. Phys. Chem. C XXXX, XXX, 000–000

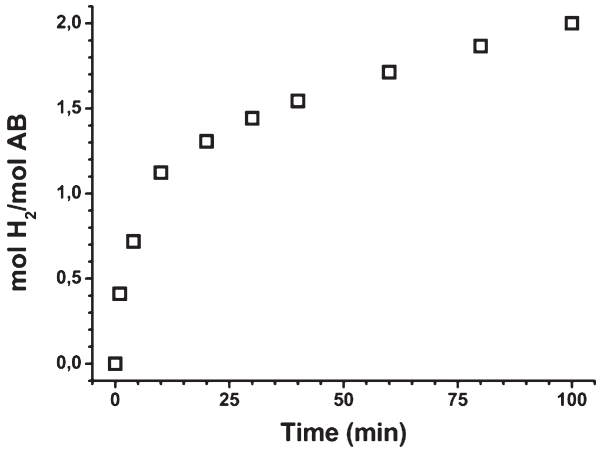

Figure 5. Volume of hydrogen generated versus time for the dehydrogenation of AB (200 mM AB) catalyzed by OAm-stabilized palladium(0) nanoclusters (2.5 mM Pd) at 25.0 ± 0.5 °C.

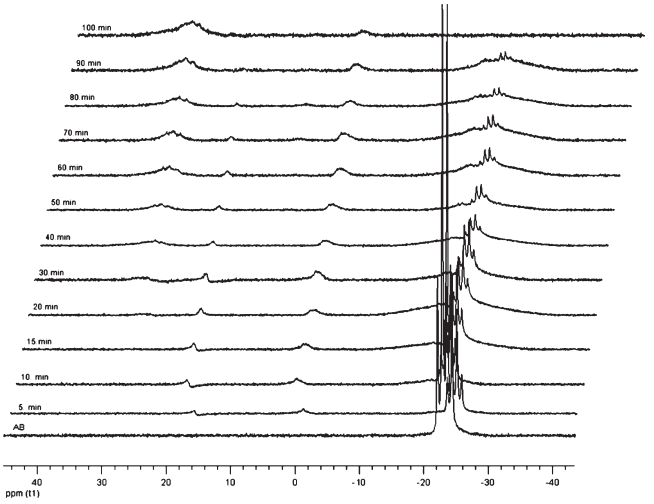

Figure 6. $^{11}B-\{^{1}H\}$ NMR spectra taken during the dehydrogenation of AB (200 mM AB) catalyzed by OAm-stabilized palladium(0) nanoclusters (2.5 mM Pd) at different reaction times at 25.0 ± 0.5 °C.

formation of cyclopolyborazane followed by polymerization to polyborazylene and (ii) through formation of long-chain linear B−N polymers. Whether the reaction proceeds in one of these two routes depends on the interaction of the AB molecule with the catalytically active site on the surface of palladium(0) nanoclusters through its nitrogen atom, B−N bond, or boron atom.[30]

Kinetics of the Dehydrogenation of AB Catalyzed by Oleylamine-Stabilized Palladium(0) Nanoclusters. To explore the kinetics of the dehydrogenation of AB catalyzed by OAm-stabilized palladium(0) nanoclusters, series of experiments were carried out by varying the ratio of stabilizer to metal, the catalyst concentration, the substrate concentration, and the reaction temperature. Figure 7 shows the plot of the hydrogen generation rate versus the [OAm]/[Pd] ratio for the dehydrogenation of AB catalyzed by OAm-stabilized palladium(0) nanoclusters at 25.0 ± 0.5 °C. As clearly seen from the Figure 7, the hydrogen generation rate increases with increasing concentration of stabilizer up to a [OAm]/[Pd] ratio of 4 and then decreases expectedly.[31] By considering both the catalytic activity

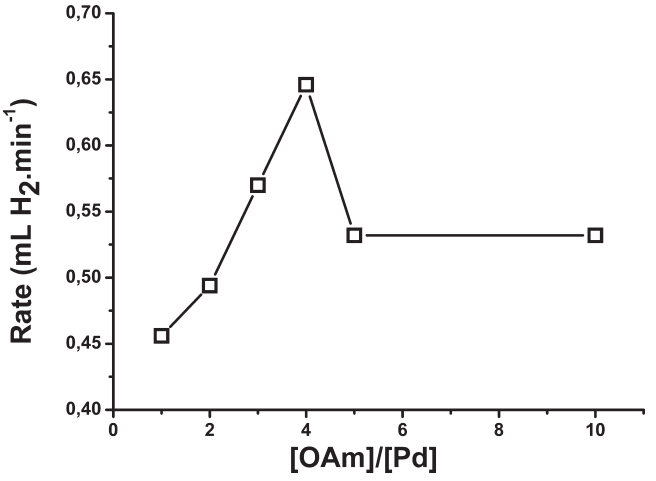

Figure 7. Plot of the hydrogen generation rate versus the [OAm]/[Pd] ratio for the dehydrogenation of AB catalyzed by OAm-stabilized palladium(0) nanoclusters at 25.0 ± 0.5 °C.

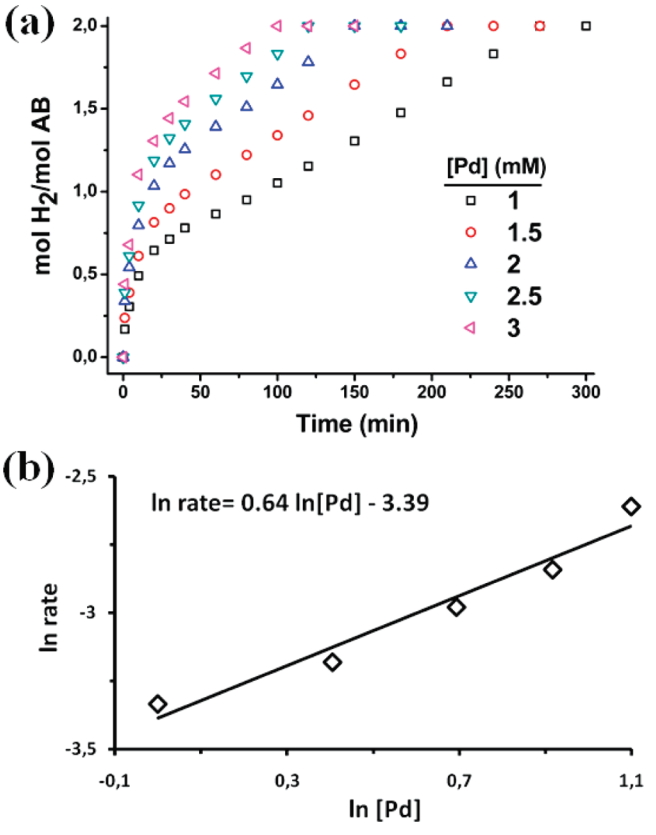

Figure 8. (a) Plots of mol H_2/mol AB versus time during the catalytic dehydrogenation of 200.0 mM AB solution in the presence of palladium(0) nanoclusters starting with different catalyst concentration (1.0−3.0 mM) at 25.0 ± 0.5 °C. (b) Plot of the hydrogen generation rate versus palladium concentration, both in logarithmic scale.

and the stability of the nanoclusters in the dehydrogenation of AB, a [OAm]/[Pd] ratio of 4 was used as the optimum ratio for all kinetic experiments.

Figure 8a shows plots of moles of H_2 per mole of AB versus time during the catalytic dehydrogenation of 200 mM AB solution

dx.doi.org/10.1021/jp201906n |J. Phys. Chem. C XXXX, XXX, 000–000

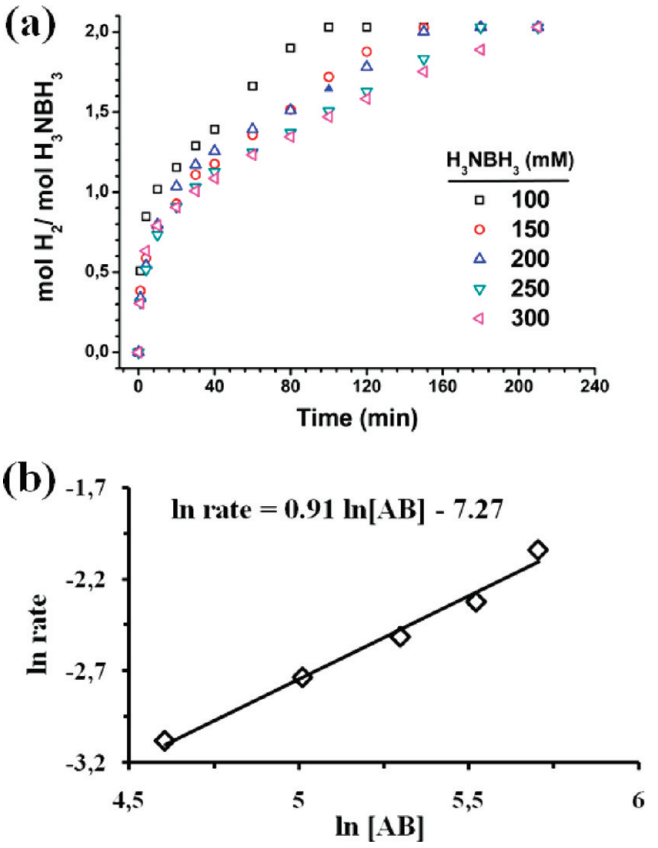

Figure 9. (a) Plots of mol H_2/mol AB versus time during the catalytic dehydrogenation of AB starting with different initial concentrations of AB while keeping the catalyst concentration constant at 2.0 mM Pd at 25.0 ± 0.5 °C. (b) Plot of the hydrogen generation rate versus AB concentration, both in logarithmic scale.

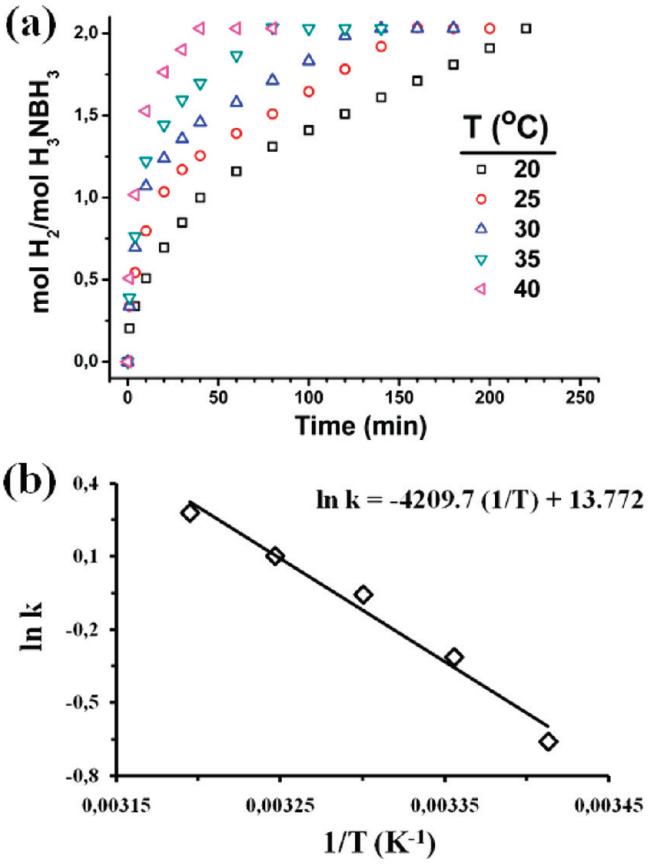

Figure 10. (a) Plots of mol H_2/mol AB versus time for the dehydrogenation of AB in the presence of OAm-stabilized palladium(0) nanoclusters at five different temperatures in the range of 20−40 °C. (b) Arrhenius plot: ln k versus $1/T$.

in the presence of palladium(0) nanoclusters starting with different catalyst concentrations in the range 1.0−3.0 mM at 25.0 ± 0.5 °C. The rate of hydrogen generation was determined from the initial, nearly linear portion of each plot for different catalyst concentrations. The hydrogen generation rate increases by increasing catalyst concentration as expected. Figure 8b shows the plot of the hydrogen generation rate versus palladium concentration, both in logarithmic scale. The line obtained has a slope of 0.64, indicating that the dehydrogenation of AB catalyzed by OAm-stabilized palladium(0) nanoclusters deviates from first-order kinetics with respect to catalyst concentration. Such a deviation might be due to the coprecipitation of some palladium(0) nanoclusters with the linear B−N polymer, a dehydrogenation product which is insoluble in the reaction medium.

The effect of substrate concentration on the dehydrogenation rate was also studied by performing a series of experiments starting with different initial concentrations of AB while keeping the catalyst concentration constant at 2.0 mM Pd at 25.0 ± 0.5 °C (Figure 9a). Plotting the hydrogen generation rate versus substrate concentration, both in logarithmic scale, gives a straight line with a slope of 0.91 (Figure 9b), indicating that hydrogen generation from the catalytic dehydrogenation of AB in the presence of OAm-stabilized palladium(0) nanoclusters is close to a first-order reaction with respect to the AB concentration. Thus, the rate law for the dehydrogenation of AB catalyzed by OAm-stabilized palladium(0) nanoclusters can be given as eq 1

$$\text{rate} = k_{app}[\text{Pd}]^{0.64}[\text{H}_3\text{NBH}_3]^{0.91} \quad (1)$$

Finally, dehydrogenation of AB catalyzed by OAm-stabilized palladium(0) nanoclusters was carried out at various temperatures in the range of 20−40 °C starting with an initial substrate concentration of 200 mM AB and an initial catalyst concentration of 2.0 mM Pd. Figure 10a shows the plots of moles of H_2 per mole of AB versus time for dehydrogenation of AB in the presence of OAm-stabilized palladium(0) nanoclusters at five different temperatures. The values of the apparent rate constant k_{app} for the catalytic dehydrogenation of AB were calculated using the rate law given in eq 1, where the rates of the reaction were determined from the initial, nearly linear portion of each plot at different temperatures. Next, they were used to draw the Arrhenius plot given in Figure 10b to calculate the apparent activation energy: $E_a^{app} = 35 \pm 2$ kJ mol^{-1}.

CS_2 Poisoning Test for the Heterogeneity of AB Dehydrogenation Catalyzed by Oleylamine-Stabilized Palladium(0) Nanoclusters. A series of poisoning experiments was carried out by adding CS_2 in varying amounts during the catalytic dehydrogenation of AB catalyzed by in-situ-generated OAm-stabilized palladium(0) nanoclusters and measuring the catalytic activity before and after addition of CS_2. Figure 11 shows the plots of volume of hydrogen generation versus time for the catalytic dehydrogenation of AB before and after addition of CS_2.

dx.doi.org/10.1021/jp201906n |J. Phys. Chem. C XXXX, XXX, 000–000

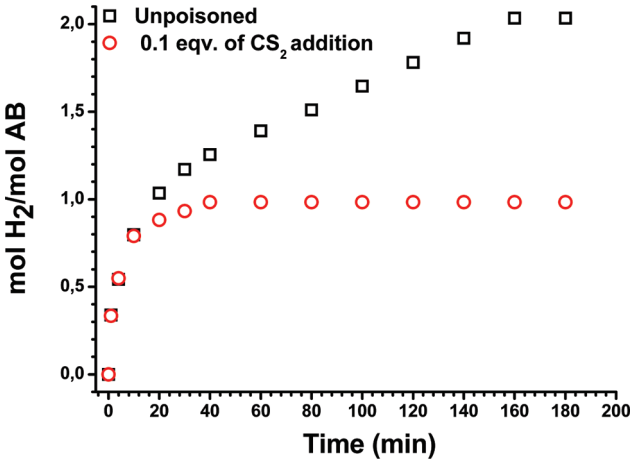

Figure 11. Plots of the volume of hydrogen generation versus time for the catalytic dehydrogenation of AB before and after addition of CS_2.

As clearly seen from Figure 11, the reaction was entirely ceased by addition of 0.1 equiv of CS_2 per Pd atom in a very short time, which indicates that the in-situ-generated OAm-stabilized palladium(0) nanoclusters act as heterogeneous catalyst in the dehydrogenation of AB.

4. CONCLUSIONS

Highly stable and redispersible palladium(0) nanoclusters were generated in situ during the dehydogenation of ammonia−borane in the presence of oleylamine and characterized by UV−vis spectroscopy, TEM, HRTEM, XRD, and FTIR methods. They were highly active catalysts in the dehydrogenation of AB, releasing 2 equiv of H_2 in 100 min with an initial TOF of 240 h^{-1} at room temperature. Ammonia−borane is eventually converted to polyborazylene by polmerization of cyclotriborazene units and insoluble linear B−N polymers in the catalytic reaction. It is also noteworthy that no detectable amount of borazine, which is a volatile compound and potential poison for fuel cell catalysts, is observed at the end of the catalytic dehydrogenation of ammonia−borane. A detailed kinetic study of the dehydrogenation of AB catalyzed by palladium(0) nanoclusters showed that it is first order with respect to the substrate concentration but deviates from first-order kinetics with respect to catalyst concentration, which might be due to coprecipitation of some palladium(0) nanoclusters with the linear B−N polymer at room temperature. To our knowledge, this is the first example of a detailed kinetic study on the dehydrogenation of ammonia−borane in the presence of heterogeneous metal catalyst.

The catalyst system described herein is palladium(0) nanoparticles stabilized by oleylamine, which has different metal−ligand interactions compared to that of rhodium(0) nanoparticles stabilized by *tert*-butylammonium octanoate, reported in our previous paper.[21] The carboxylate anion appears to be an excellent stabilizer for Rh and Ir. However, for palladium(0) nanoparticles, amines are efficient stabilizers. Oleylamine is unique for stabilizing palladium(0) nanoclusters without lowering the catalytic activity. The difference in the metal−ligand interaction also has the consequence that Rh nanoclusters stabilized by carboxylate anion can release 1.4 equiv of hydrogen while Pd nanoclusters stabilized by oleylamine generate 2 equiv of hydrogen from the dehydrogenation of AB at room temperature. Another advantage is the ease of preparation of the catalyst system reported in the current work. Rh nanoclusters were ex-situ prepared from the reduction of Rh(II) octanoate by *tert*-butylamine−borane using difficult experimental steps. In contrast, the oleylamine-stabilized Pd nanoclusters were in-situ generated during the catalytic dehydrogenation of AB, and hydrogen generation starts immediately after formation of the palladium nanoclusters.

AUTHOR INFORMATION

Corresponding Author

*Phone: +90 312 210 3212, Fax: +90 312 210 3200. E-mail: sozkar@metu.edu.tr.

Present Addresses

† Department of Chemistry, Atatürk University, 25240 Erzurum, Turkey.

‡ On the leave from the Department of Chemistry, Bingöl University, 12400 Bingöl, Turkey.

ACKNOWLEDGMENT

Partial support by the Turkish Academy of Sciences and TUBİTAK (Research Fellowship-2218 for S.D.) is gratefully acknowledged. Ö.M. thanks to the METU-DPT-OYP program on the behalf of Atatürk University.

REFERENCES

(1) U.S. Department of Energy, Office of Energy Efficiency and Renewable Energy and The FreedomCAR and Fuel Partnership, Targets for Onboard Hydrogen Storage Systems for Light-duty Vehicles, September 2009, available at http://www.eere.energy.gov.

(2) Schlapbach, L.; Züttel, A. *Nature* **2001**, *414*, 353–358.

(3) Hamilton, C. W.; Baker, R. T.; Staubitz, A.; Manners, I. *Chem. Soc. Rev.* **2009**, *38*, 279.

(4) (a) Marder, T. B. *Angew. Chem., Int. Ed.* **2007**, *46*, 8116–8118. (b) Stephens, F. H.; Pons, V.; Baker, R. T. *Dalton Trans.* **2007**, *25*, 2613–2626and references therein.

(5) (a) Baitalow, F.; Baumann, J.; Wolf, G.; Jaenicke, K.; Leitner, G. *Thermochim. Acta* **2002**, *391*, 159–168. (b) Wolf, G.; Baumann, J.; Baitalow, F.; Hoffman, F. P. *Thermochim. Acta* **2000**, *343*, 19–25.

(6) Erdogan, H.; Metin, Ö.; Özkar, S. *Phys. Chem. Chem. Phys.* **2009**, *11*, 10519–10525.

(7) Xu, Q.; Chandra, M. J. *Alloys Compd.* **2007**, *446−447*, 729–732.

(8) (a) Jaska, C. A.; Temple, K.; Lough, A. J.; Manners, I. *Chem. Commun.* **2001**, 962–963. (b) Denney, M. C.; Pons, V.; Hebden, T. J.; Heinekey, D. M.; Goldberg, K. I. *J. Am. Chem. Soc.* **2006**, *128*, 12048–12049.

(9) Hamilton, C. W.; Baker, R. T.; Staubitz, A.; Manners, I. *Chem. Soc. Rev.* **2009**, *38*, 279–293.

(10) (a) Davis, B. L.; Dixon, D. A.; Garner, E. B.; Gordon, J. C.; Matus, M. H.; Scott, B.; Stephens, F. H. *Angew. Chem., Int. Ed.* **2009**, *48*, 6812–6816. (b) Mock, M. T.; Potter, R. G.; Camaioni, D. M.; Li, J.; Dougherty, W. G.; Kassel, W. S.; Twamley, B.; DuBois, D. L. *J. Am. Chem. Soc.* **2009**, *131*, 14454–14465.

(11) (a) Jiang, Y.; Berke, H. *Chem. Commun.* **2007**, 3571–3573. (b) Jaska, C. A.; Temple, K.; Lough, A. J.; Manners, I. *J. Am. Chem. Soc.* **2003**, *125*, 9424–9434. (c) Jaska, C. A.; Manners, I. *J. Am. Chem. Soc.* **2004**, *126*, 9776–9785. (d) Chen, Y.; Fulton, J. L.; Linehan, J. C.; Autrey, T. *J. Am. Chem. Soc.* **2005**, *127*, 3254–3255. (e) Fulton, J. L.; Linehan, J. C.; Autrey, T.; Balasubramanian, M.; Chen, Y.; Szymczak, N. K. *J. Am. Chem. Soc.* **2007**, *129*, 11936–11949. (f) Clark, T. J.; Russell, C. A.; Manners, I. *J. Am. Chem. Soc.* **2006**, *128*, 9582–9583. (g) Pun, D.; Lobkovsky, E.; Chirik, P. J. *Chem. Commun.* **2007**, 3297–3299.

(12) (a) Jaska, C. A.; Temple, K.; Lough, A. J.; Manners, I. *J. Am. Chem. Soc.* **2003**, *125*, 9424–9434. (b) Jaska, C. A.; Manners, I. *J. Am. Chem. Soc.* **2004**, *126*, 1334–1335.
(13) Denney, M. C.; Pons, V.; Hebden, T. J.; Heinekey, M.; Goldberg, K. I. *J. Am. Chem. Soc.* **2006**, *128*, 12048–12049.
(14) (a) Blaquiere, N.; Diallo-Garcia, S.; Gorelsky, S. I.; Black, D. A.; Fagnou, K. *J. Am. Chem. Soc.* **2008**, *130*, 14034–14035. (b) Käss, M.; Friedrich, A.; Drees, M.; Schneider, S. *Angew. Chem., Int. Ed.* **2009**, *48*, 905–907.
(15) Keaton, R. J.; Blacquiere, J. M.; Baker, R. T. *J. Am. Chem. Soc.* **2007**, *129*, 1844–1845.
(16) Kim, S.-K.; Han, W.-S.; Kim, T.-J.; Kim, T.-Y.; Nam, S. W.; Mitoraj, M.; Piekos, L.; Michalak, A.; Hwang, S.-J.; Kang, S. O. *J. Am. Chem. Soc.* **2010**, *132*, 9954–9955.
(17) Shrestha, R. P.; Diyabalanage, H. V. K.; Semelsberger, T. A.; Ott, K. C.; Burrell, A. K. *Int. J. Hydrogen Energy* **2009**, *34*, 2616–2621.
(18) Özkar, S. *Appl. Surf. Sci.* **2009**, *256*, 1272–1277.
(19) Roucoux, A.; Schulz, J.; Patin, H. *Chem. Rev.* **2002**, *102*, 3757–3778.
(20) Aiken, J. D.; Finke, R. G. *J. Mol. Catal. A: Chem.* **1999**, *145*, 1–44.
(21) Ayvalı, T.; Zahmakıran, M.; Özkar, S. *Dalton Trans.* **2011**, *40*, 3584–3591.
(22) Mazumder, V.; Sun, S. *J. Am. Chem. Soc.* **2009**, *131*, 4588–4589.
(23) Creighton, J. A.; Eadon, D. G. *J. Chem. Soc., Faraday Trans.* **1991**, *87*, 3881–3891(Nanometer-sized metal clusters exhibit unique optical properties. For instance, Au, Ag, and Cu nanoparticles exhibit a strong surface plasmon resonance that is superimposed onto the exponential-decay Mie-scattering spectra. However, for nanometer-sized Pd particles, the absorption profile does not feature a well-defined surface-plasmon band; instead, for particles within the size range obtained above, only the Mie scattering spectra can be observed.).
(24) Chen, S.; Huang, K.; Stearns *J. A. Chem. Mater.* **2000**, *12*, 540–547.
(25) Face centered cubic palladium, Joint Committee on Powder Diffraction Studies (JCPDS) card No: 46-1043, 1969.
(26) Liu, Y.; Wang, C.; Wei, Y.; Zhu, L.; Li, D.; Jiang, J. S.; Markovic, N. M.; Stamenkovic, V. R.; Sun, S. *Nano Lett.* **2011**, *11*, 1614–1617.
(27) Rioux, R. M.; Song, H.; Yang, P.; Somorjai, G. A. *Metal Nanoclusters in Catalysis and Materials Science: The Issue of Size Control*; Corain, B., Schmid, G., Toshima, N., Eds.; Elsevier: Netherlands, 2008; Chapter 7.
(28) See the Table S1 in the Supporting Information of our recent published paper given in ref 22.
(29) Smythe, N. C.; Gordon, J. C. *Eur. J. Inorg. Chem.* **2010**, 509–521.
(30) Pons, V.; Baker, R. T.; Szymczak, N. K.; Heldebrant, D. J.; Linehan, J. C.; Matus, M. H.; Grant, D. J.; Dixon, D. A. *Chem. Commun.* **2008**, 6597–6599.
(31) Watzky, M. A.; Finke, R. G. *J. Am. Chem. Soc.* **1997**, *119*, 10382–10400.